# Auger-Electron Spectroscopy of Transition Metals

T. W. Haas, J. T. Grant, and G. J. Dooley
*Aerospace Research Laboratories, Wright-Patterson Air Force Base, Ohio 45433*
(Received 13 October 1969)

The Auger-electron spectra in the intermediate- and low-energy range (0–1 keV) for many of the transition metals of periods 4–6 (specifically, Sc, Ti, V, Cr, Fe, Co, Y, Zr, Nb, Mo, Ru, Rh, La, Hf, Ta, W, Re, Ir, Pt, and Au) have been measured. In general, the spectra from elements in the same period of the Periodic Table are similar, the main difference being the energy at which the Auger electrons appear. The main transitions observed from period-4 elements are of the *LMM* type. For period-5 elements, the Auger transitions involve *MNN* levels, and for the period-6 elements, the transitions are of the *NNN* (Coster-Kronig) type.

## I. INTRODUCTION

An electron incident on a metal surface may interact with it in a number of ways. This interaction can be characterized as inelastic or elastic scattering according to whether the internal state of the scatterer is changed or not. In the case of elastic scattering of electrons of low energy (0–500 eV) from single crystal surfaces, it is known that diffraction (LEED) can be used to gain structural information.[1] The use of the display-type LEED instrument has lately been modified to give measurements of the energy distributions of inelastically scattered electrons as well.[2,3] Among the many inelastic scattering channels available, attention has focused mainly on those involving excitation of plasmons[2–4] and on the Auger effect.[5–13] This latter mechanism has been shown capable of giving valuable information on qualitative and semiquantitative analysis of trace contaminants on surfaces, as well as the potential for determining chemical (valence) states of surface atoms via chemical shift measurements.[14]

A number of Auger spectra have been published and certain trends suggested. There are many transitions possible for heavy atoms, but which will be the most important for Auger spectroscopy has not been established. It has been suggested that an atlas of Auger spectra should be compiled.[12] Part of the purpose of this paper was to provide such information for most of the transition metals in periods 4–6 of the Periodic Table, excepting mainly the rare earths. Specifically, spectra are presented from Sc, Ti, V, Cr, Fe, Co, Y, Zr, Nb, Mo, Ru, Rh, La, Hf, Ta, W, Re, Ir, Pt, and Au. The indexing of the observed transitions is facilitated by the trends which are observed along periods in the periodic chart. Critical excitation energies as well as chemical effects are also found useful for this purpose.

## II. EXPERIMENTAL

The Auger spectrometers used were Varian 3- and 4-grid LEED systems operated as retarding potential energy analyzers.[2,15] The second derivative of current to the screen versus the energy of the inelastic electrons was generally recorded, although in some cases the first derivative was also measured. In many cases, the LEED gun was used as the electron source, but a side gun such as suggested by Palmberg[15] was also used. The features of the spectra obtained from essentially clean surfaces were not dependent on which gun was used. Incident beam voltages were between 200 V and 2.5 kV and currents were from 2 to 200 $\mu$A. Modulating signals applied to the suppressor grid were generally 140 Hz and 2 V rms unless fine structure was observed, in which case lower amplitudes were used. In all cases, a suppressor voltage-sweep speed in sec/V was selected which was three or four times less than the time constant of the lock-in amplifier; experience shows that this is generally sufficient to avoid anomalous shifts of peaks.

In nearly all cases, one measurements was made with a positive voltage applied to the sample. This technique shifts the Auger peaks to lower voltages on the suppressor scale by the amount of the voltage applied to the sample. This was done primarily to assure that no extraneous peaks were being included at very high gains, as any peaks not shifted in this way cannot be from the sample. The high-energy Auger peaks from Fe and Co were also measured in this manner.

The materials used in this study were all high-purity foils or, in some cases, oriented single-crystal specimens. The only exception was the Hf foil, which contained 3% of Zr.

## III. RESULTS

### A. Surface Cleaning

Auger spectra were obtained from the samples after bake out of the chamber and before any additional

[1] J. J. Lander, Progr. Solid State Chem. **2**, 26 (1965).
[2] E. J. Scheibner and L. N. Tharp, Surface Sci. **8**, 247 (1967).
[3] L. N. Tharp and E. J. Scheibner, J. Appl. Phys. **38**, 3320 (1967).
[4] T. W. Haas, J. Appl. Phys. **39**, 5854 (1968).
[5] P. Auger, Compt. Rend. **180**, 65 (1925); **182**, 973 (1926).
[6] J. J. Lander, Phys. Rev. **91**, 1382 (1953).
[7] L. A. Harris, J. Appl. Phys. **39**, 1419 (1968); **39**, 1428 (1968).
[8] R. E. Weber and W. T. Peria, J. Appl. Phys. **38**, 4355 (1967).
[9] P. W. Palmberg, J. Appl. Phys. **38**, 2137 (1967).
[10] P. W. Palmberg and T. N. Rhodin, J. Appl. Phys. **39**, 2425 (1968).
[11] R. E. Weber and A. L. Johnson, J. Appl. Phys. **40**, 314 (1969).
[12] H. E. Bishop and J. C. Riviere, J. Appl. Phys. **40**, 7240 (1969).
[13] N. J. Taylor, Rev. Sci. Instr. **40**, 792 (1969).
[14] T. W. Haas and J. T. Grant, Phys. Letters **30A**, 272 (1969).
[15] P. W. Palmberg, Appl. Phys. Letters **13**, 183 (1968).

TABLE I. Auger transitions observed in the intermediate-energy range from period-6 transition metals. Equivalent features labeled a, b, and c are identified in Fig. 1(b). The $Z$ column refers to calculated energies using the ground-state binding energies, the $Z+1$ refers to Eq. (2), and the $\Delta Z$ column refers to Eq. (4) with $\Delta Z=0.7$. All energies are given in eV.

| Feature | a | | | | b | | | | c | | | |
|---|---|---|---|---|---|---|---|---|---|---|---|---|
| Transition | $N_V N_{VI} N_{VI}$ | | | | $N_V N_{VI} N_{VII}$ | | | | $N_V N_{VII} N_{VII}$ | | | |
| At. No./ Element | Expt | $Z$ | $Z+1$ | $\Delta Z$ | Expt | $Z$ | $Z+1$ | $\Delta Z$ | Expt | $Z$ | $Z+1$ | $\Delta Z$ |
| 72 Hf | 168 | 176 | 166 | 169 | 172 | 177 | 170 | 172 | 180 | 178 | 171 | 173 |
| 73 Ta | 168 | 176 | 166 | 169 | 173 | 178 | 169 | 172 | 181 | 180 | 171 | 174 |
| 74 W | 164 | 172 | 162 | 165 | 171 | 175 | 164 | 168 | 181 | 178 | 167 | 170 |
| 75 Re | 163 | 166 | 161 | 163 | 170 | 168 | 163 | 165 | 180 | 170 | 165 | 167 |
| 77 Ir | 158 | 169 | 158 | 161 | 164 | 172 | 162 | 165 | 174 | 175 | 165 | 168 |
| 78 Pt | 152 | 166 | 153 | 157 | 160 | 170 | 157 | 161 | 172 | 174 | 161 | 163 |
| 79 Au | 144 | 160 | 144 | 149 | 156 | 164 | 148 | 153 | 164 | 168 | 152 | 157 |

cleaning procedure was attempted. In most cases, these spectra were of very low intensity, and it was necessary to heat the samples to at least 500°C to obtain usable spectra. In order to obtain results characteristic of the metal, attempts were made to remove all surface contaminants to below detectable levels. Several techniques were employed for this purpose and all are fairly well known.[16] Generally, Ar-ion bombardment, high-temperature anneal (to near the melting point), reaction with H or O, or evaporation on to a substrate were the techniques employed. In some cases, it appears as though an atomically clean surface is almost impossible to obtain. In particular, the Zr and O could never be fully removed from Hf, and O always seemed to be present on Ti and Zr, and possibly V and Cr. The levels of these impurities were low, however, and probably had little effect on the results except for a minor shift in voltage due to chemical effects.[14] The presence of these impurities could be detected after ion bombarding the surface and comparing relative peak heights before and after annealing. For example, with Y, one of the principal impurities is Cl, which is not detected on the bombarded unannealed surface but does reappear after annealing. Many of the contaminants found on these metals during cleaning, as well as techniques for their removal, have been reviewed elsewhere.[17]

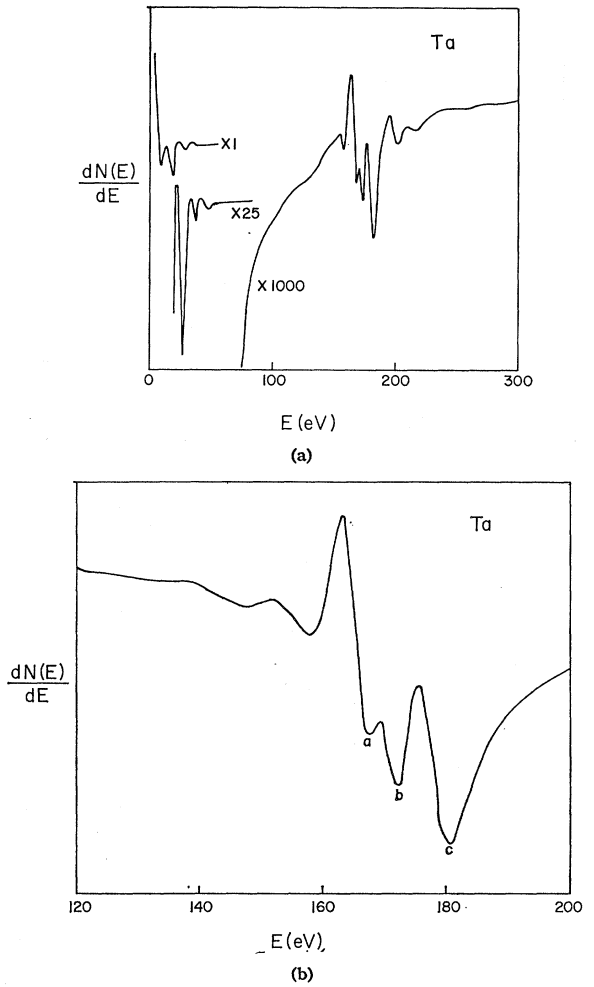


FIG. 1. (a) Auger electron spectrum from Ta(110) crystal in the low- and intermediate-energy range. Relative gains are indicated by the amplification factors shown by each curve. (b) Expanded section of Auger electron spectrum from Ta. Features labeled a, b, and c are referred to in text and Table I.

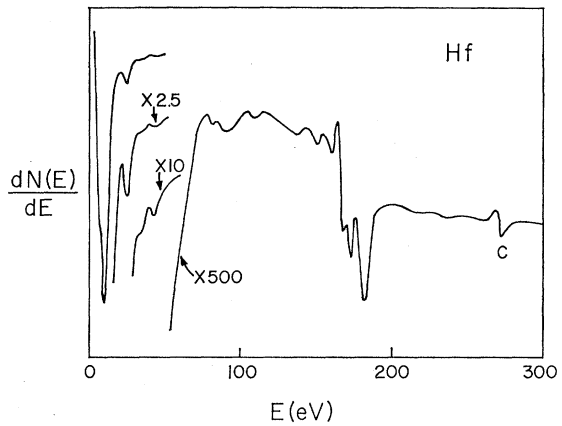


FIG. 2. Auger electron spectrum from Hf foil after ion bombardment. Note presence of peak at 270 eV due to C. A peak of similar size appears at 510 eV due to O indicating CO had chemisorbed on the surface during bombardment.

[16] R. W. Roberts, Brit. J. Appl. Phys. **14**, 537 (1963).
[17] T. W. Haas, J. T. Grant, and G. J. Dooley, J. Vac. Sci. Technol. (to be published).

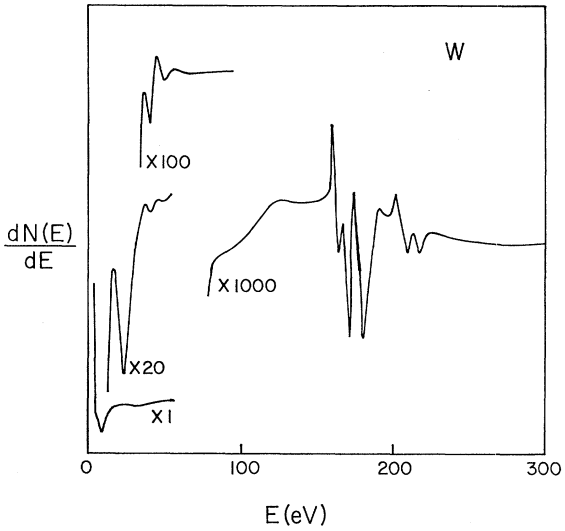


FIG. 3. Auger electron spectrum from W foil.

### B. General Features of Auger Spectra

The first, and perhaps most striking, result is the similarity of the spectra obtained from metals in the same period in the periodic chart. For example, the major feature in the Ta spectrum for energies less than 1 keV, apart from the low-energy (<50-eV) peaks, is a characteristic line shape with a first maximum at 164 eV [Fig. 1(a)]. An expanded section of this spectrum is shown in Fig. 1(b). It should be noted that the several sharp maxima in this feature are obscured if a modulating voltage of more than 2 V rms is used. On the other hand, the use of smaller modulating voltages does not bring out additional features. This same line shape is observed in the spectra of all the period-6 metals studied, viz., Hf, Ta, W, Re, Ir, Pt, and Au, with the exception of La. Spectra from Hf, Ta, W, Re, Ir, Pt, and Au are given in Figs. 1–7. (Spectra from Au, W, and Pt have been published previously and our results are in substantial agreement with previously published spectra. For consistency, energies given for the various transitions in Table I are all taken from our work.) A monotonic decrease in the energy at which this Auger feature appears is observed for these period-6 elements as the atomic number increases. Thus, this first maximum appears at 165 eV for Hf and decreases to 139 eV for Au. The data from these period-6 metals are summarized in Table I. In this table, the features referred to are identified by a, b, and c in Fig. 1(b).

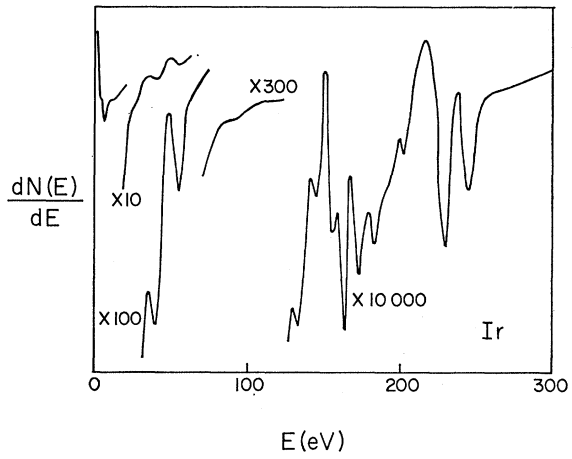


FIG. 5. Auger electron spectrum from Ir (100) crystal.

La is somewhat different from the rest of the period-6 materials presented here in that it has vacancies in the inner $4f$ shells. Its spectrum, given in Fig. 8, is similar to that of Cs,[8] which is closer in atomic number than are the other period-6 elements studied here.

The period-4 elements also were observed to give similar spectra to each other. In this case, a characteristic three-line feature is observed which under high

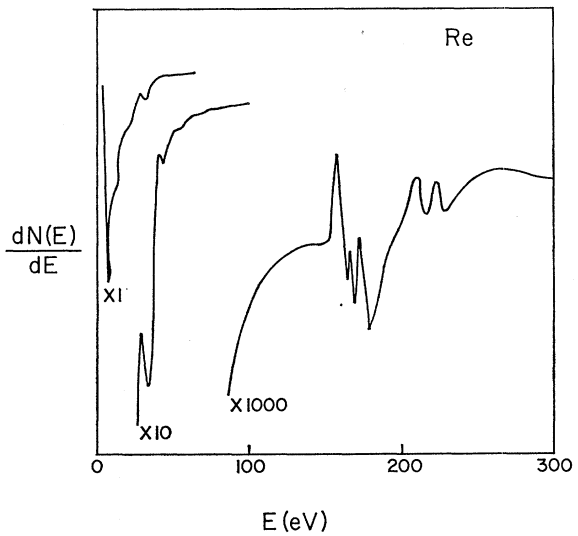


FIG. 4. Auger electron spectrum from Re foil.

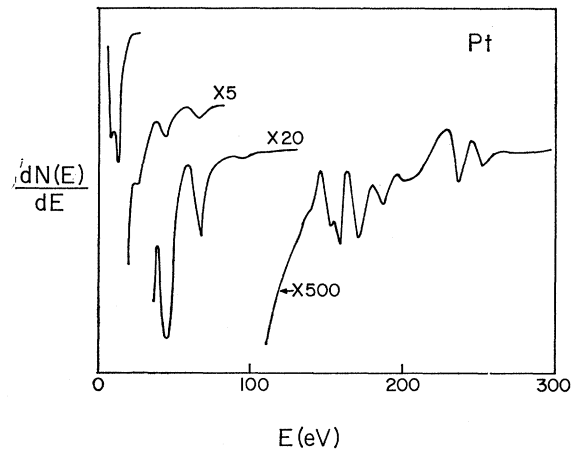


FIG. 6. Auger electron spectrum from Pt (100) crystal.

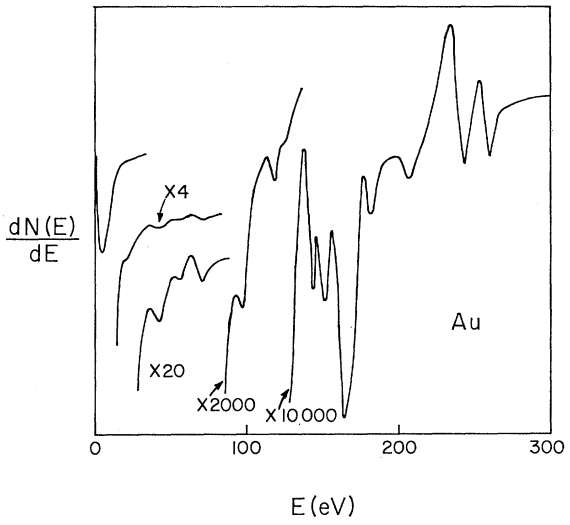


FIG. 7. Auger electron spectrum from Au foil.

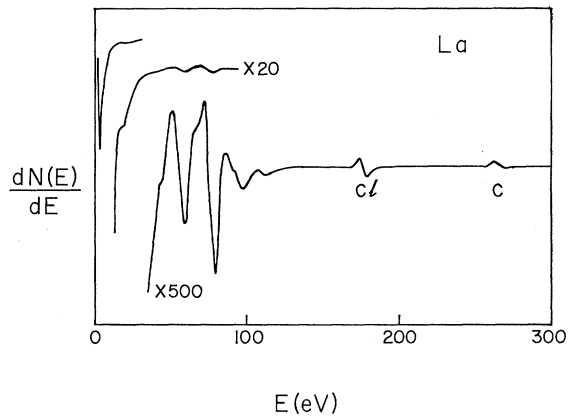


FIG. 8. Auger electron spectrum from La foil. Note presence of peaks due to Cl and C identified in figure. A peak due to O at 510 eV (not shown) was also found of comparable size to the Cl peak.

resolution is found to contain fine structure. The spectra of Sc, Ti, V, Cr, and Co are given in Figs. 9–13. For the elements in this period, this "triplet" occurs at higher energies as the atomic number increases. The results are summarized in Table II with again the corresponding features labeled as in Fig. 11. It should be noted that the relative heights of the three "lines" is not constant from Sc to Co.

A somewhat different behavior is observed from the elements in period 5. The spectra from Y, Zr, Nb, and Mo are again very similar in shape, with only shifts in energy, but a slight change in shape occurs between Mo and Ru. The features of the spectra from Ru, Rh, Pd,[10] and Ag[10] are again similar with only energy shifts between them. In this case, it is also observed that the Auger electrons have higher energies as elements of higher atomic number are measured. The Auger spectra from Y, Zr, Nb, Mo, Ru, and Rh are given in Figs. 14–19. From these figures, one can see that the principal change in spectra is in the relative heights of the peaks rather than in their number or spacing. These results are summarized in Table III and corresponding features are identified in Fig. 16(b).

It can be seen from these results that for periods 4 and 5 the energies at which the characteristic line shapes occur increase with atomic number whereas for period 6 the energies decrease.

Finally, we note that the comparison of these Auger spectra has centered mainly on those Auger features in the intermediate-energy range, i.e., 50–1000 eV. There are strong features also observed in the true secondary region, (<50 eV) but these are frequently found in regions where there is high background and, hence, are

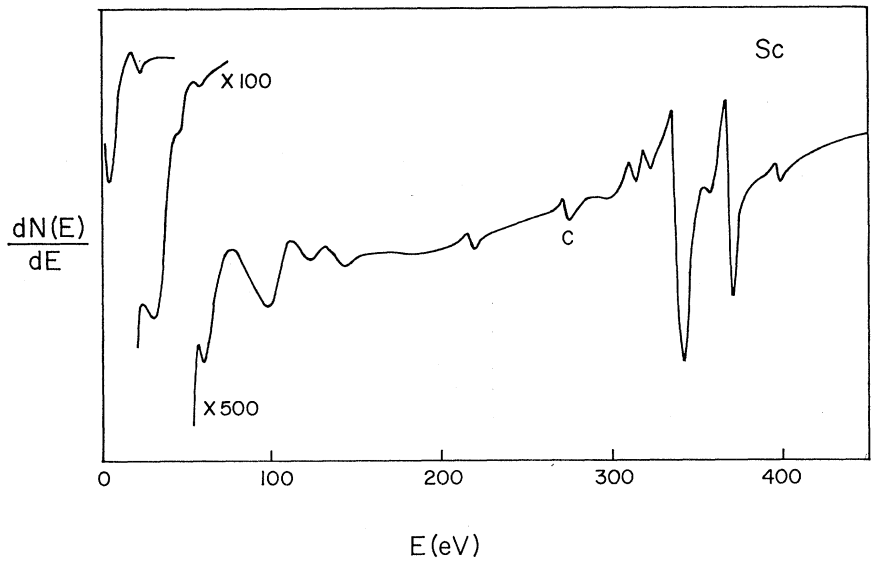


FIG. 9. Auger electron spectrum from Sc foil. Note presence of peak due to C. A peak of similar size due to O was also found at 510 eV (not shown).

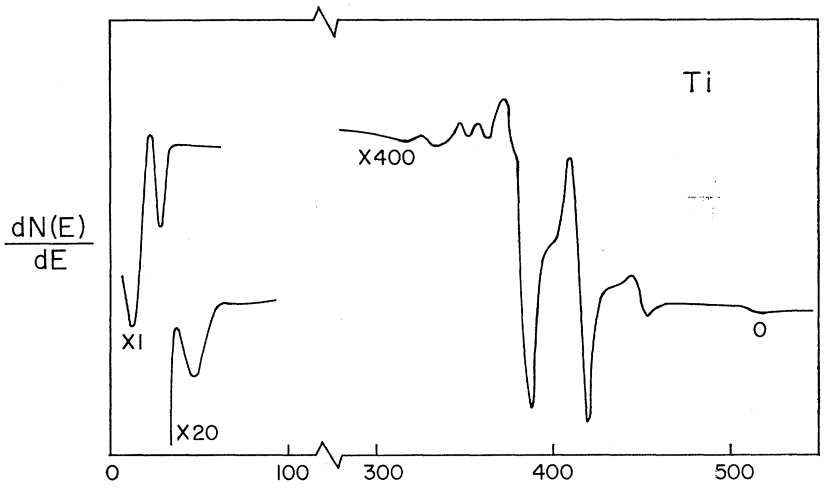


FIG. 10. Auger electron spectrum from Ti foil after Ar-ion bombardment. Note presence of peak at 510 eV due to O.

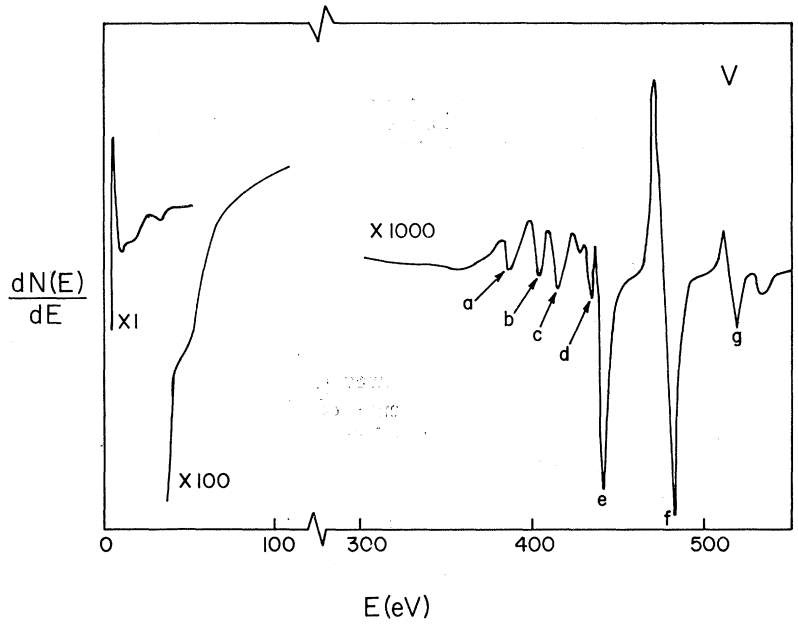


FIG. 11. Auger electron spectrum from V foil. Features labeled a, b, c, etc. are discussed in text and in Table II.

TABLE II. Auger transitions observed in the intermediate-energy range from period-4 elements. Equivalent features labeled a, b, etc. are identified in Fig. 11. The $Z$ column refers to calculated energies using the ground-state binding energies, while the $Z+1$ column refers to values calculated from Eq. (2). All energies are given in eV.

| Feature | a | | | b | | | c | | | d | | | e | | | f | | | g | | |
|---|---|---|---|---|---|---|---|---|---|---|---|---|---|---|---|---|---|---|---|---|---|
| Transition | $L_{II}M_IM_I$ | | | $L_{III}M_IM_{III}$ | | | $L_{II}M_IM_{III}$ | | | $L_{III}M_{III}M_{III}$ | | | $L_{II}M_{III}M_{III}$ | | | $L_{II}M_{III}M_V$ | | | $L_{II}M_VM_V$ | | |
| At. No./ Element | Expt | $Z$ | $Z+1$ | Expt | $Z$ | $Z+1$ | Expt | $Z$ | $Z+1$ | Expt | $Z$ | $Z+1$ | Expt | $Z$ | $Z+1$ | Expt | $Z$ | $Z+1$ | Expt | $Z$ | $Z+1$ |
| 21 Sc | 294 | 299 | 294 | 307 | 316 | 314 | 316 | 321 | 319 | 331 | 338 | 336 | 338 | 343 | 341 | 371 | 368 | 372 | 400 | 393 | 397 |
| 22 Ti | 327 | 343 | 336 | 350 | 362 | 358 | 361 | 368 | 364 | 373 | 387 | 383 | 380 | 393 | 389 | 418 | 424 | 425 | 452 | 455 | 456 |
| 23 V | 386 | 388 | 380 | 402 | 409 | 404 | 412 | 416 | 411 | 431 | 437 | 432 | 438 | 444 | 439 | 475 | 480 | 480 | 510 | 516 | 516 |
| 24 Cr | NR[a] | 436 | 426 | NR | 458 | 452 | NR | 467 | 461 | NR | 499 | 493 | 490 | 492 | 492 | 530 | 539 | 537 | 575 | 580 | 578 |
| 26 Fe | 522 | 533 | 527 | 557 | 559 | 555 | 569 | 572 | 568 | 597 | 598 | 594 | 605 | 611 | 607 | 655 | 661 | 664 | 710 | 711 | 714 |
| 27 Co | 580 | 592 | 581 | 610 | 618 | 610 | 625 | 633 | 625 | 650 | 659 | 651 | 660 | 674 | 666 | 720 | 731 | 730 | 780 | 784 | 783 |
| 28 Ni[b] | NR | 648 | 640 | NR | 675 | 669 | NR | 678 | 672 | NR | 719 | 712 | 720 | 736 | 730 | 790 | 796 | 798 | 860 | 864 | 866 |
| 29 Cu[b] | NR | 711 | 694 | NR | 737 | 724 | NR | 757 | 744 | NR | 783 | 770 | 795 | 803 | 790 | 875 | 875 | 868 | 950 | 947 | 940 |

[a] NR signifies not resolved.

[b] Experimental values taken from Ref. 10.

TABLE III. Auger transitions observed in the intermediate-energy range from period-5 transition metals. Equivalent features labeled a, b, etc. are identified in Fig. 16(b). The $Z$ column refers to calculated energies using the ground-state binding energies, while the $Z+1$ column refers to values calculated from Eq. (2). All energies are given in eV.

| Feature | a | | | b | | | c | | | d | | | e | | |
|---|---|---|---|---|---|---|---|---|---|---|---|---|---|---|---|
| Transition | $M_V N_I N_{III}$ | | | $M_V N_{III} N_{III}$ | | | $M_V N_I N_V$ | | | $M_V N_{III} N_V$ | | | $M_V N_V N_V$ | | |
| At. No./ Element | Expt | $Z$ | $Z+1$ | Expt | $Z$ | $Z+1$ | Expt | $Z$ | $Z+1$ | Expt | $Z$ | $Z+1$ | Expt | $Z$ | $Z+1$ |
| 39 Y | 79 | 85 | 82 | 101 | 106 | 103 | 109 | 109 | 109 | 129 | 129 | 129 | 149 | 152 | 152 |
| 40 Zr | 93 | 99 | 94 | 117 | 123 | 118 | 127 | 125 | 124 | 149 | 148 | 147 | 175 | 174 | 173 |
| 41 Nb | 108 | 113 | 112 | 134 | 137 | 138 | 145 | 143 | 145 | 169 | 167 | 169 | 199 | 197 | 199 |
| 42 Mo | 125 | 130 | 126 | 153 | 157 | 153 | 166 | 163 | 163 | 192 | 190 | 190 | 226 | 223 | 223 |
| 44 Ru | 156 | 161 | 156 | 190 | 193 | 188 | 206 | 202 | 201 | 237 | 234 | 233 | 280 | 275 | 274 |
| 45 Rh | 174 | 178 | 175 | 208 | 211 | 208 | 226 | 223 | 225 | 260 | 256 | 258 | 306 | 301 | 303 |
| 46 Pd[a] | | | | | | | 250 | 248 | 246 | 285 | 283 | 281 | 337 | 333 | 331 |
| 47 Ag[a] | | | | | | | 268 | 269 | 263 | 308 | 308 | 302 | 362 | 364 | 358 |

[a] Experimental values taken from Ref. 10.

found as shoulders in the spectra. Some trends in these spectra are found as can be seen in Table IV.

### C. Yields and Critical Ionization Energies

It is very difficult to make quantitative comparisons of yields of Auger electrons per incident electron for the metals studied because of various experimental problems. For example, surface roughness will vary from sample to sample and so will microscopic flatness (which will affect angles of incidence). There is also some difficulty in obtaining a reproducible current density from the electron gun to the degree necessary for comparative yield measurements. However, it is possible to make some estimates of the yields. For period-5 or period-6 elements, the yields apparently do not vary by more than a factor of about 2. However, there is a difference in yields between elements of these two periods. The yields from period-6 elements are consistently smaller than those of period 5 by a factor of about 3–5. The Auger electrons of interest here are in the same energy range (150–350 eV), so such a comparison has some validity. Estimates for period-4 elements are more difficult, as the triplet of peaks observed is found over a wide range of energy (350–400 eV for Sc to 800–1000 eV for Cu). Comparative measurements in this case would require a very high incident-beam energy to minimize backscatter, etc.

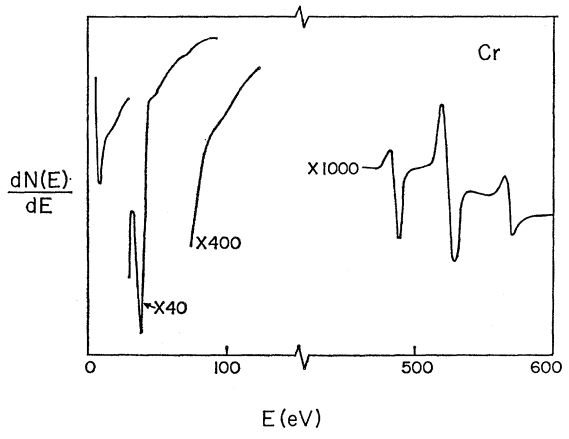


FIG. 12. Auger electron spectrum from Cr (110) crystal.

Yields as a function of angle of incidence may show maxima and minima related to the type of Bloch waves excited in the crystal.[18,19] Some effort was made to detect such effects from single-crystal metal samples for beams at near-normal incidence, but any changes were very small. There seemed to be no correlation in yield with the brightness of the various diffracted beams.

Yields as a function of incident-beam voltage can yield important information about both backscatter and critical ionization energies. Houston and Park[20] have given some data on the yield of one of the Ni peaks as a function of voltage and conclude that backscatter can be important in determining yields. In Fig. 20, data

TABLE IV. Energies of main Auger transitions observed in the secondary region (<50 eV) for transition metals in periods 4–6.

| Element | Auger electron energies | | | |
|---|---|---|---|---|
| Sc | 24 | 36 | | |
| Ti | 12 | 28 | 47 | |
| V | 9 | 14 | 32 | 48 |
| Cr | 14 | 37 | 47 | |
| Fe | 14 | 25 | 48 | |
| Co | 14 | 54 | | |
| Y | 20 | 28 | | |
| Zr | 23 | 34 | 47 | |
| Nb | 16 | 26 | 37 | |
| Mo | 20 | 28 | 40 | |
| Ru | 15 | 37 | 48 | |
| Rh | 14 | 28 | 42 | |
| La | 23 | | | |
| Hf | 10 | 25 | 33 | 43 |
| Ta | 17 | 27 | 36 | 46 |
| W | 12 | 24 | 40 | 50 |
| Re | 12 | 20 | 34 | 45 |
| Ir | 12 | 25 | 41 | |
| Pt | 12 | 24 | 43 | |
| Au | 24 | 44 | | |

[18] P. Duncumb, Phil. Mag. **7**, 201 (1963).
[19] P. D. Hirsch, A. Howie, and M. J. Whelan, Phil. Mag. **7**, 2095 (1962).
[20] J. E. Houston and R. L. Park, Appl. Phys. Letters **14**, 358 (1969).

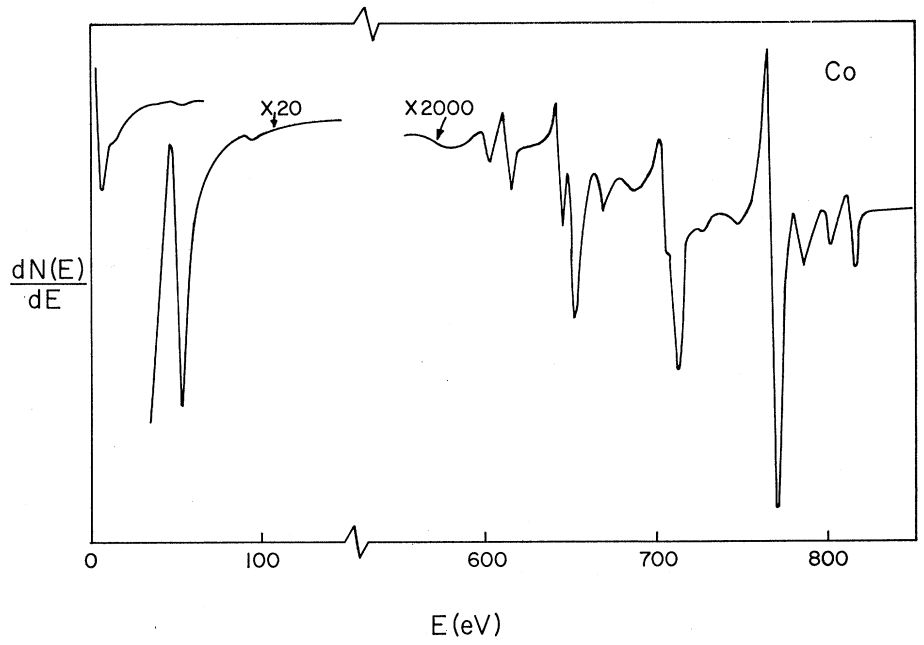


FIG. 13. Auger electron spectrum from Co foil.

on the yield of the Ta 164-eV Auger peak as a function of primary beam energy is given. The yield is arbitrarily defined as the peak-to-peak deflection from the maximum at 164 eV to the minimum at 181 eV and is normalized for change in incident-beam current. The sample was a clean Ta (110) single crystal. It can be seen that this transition can be excited by incident electrons of less than 285 eV. It may be possible to excite this transition with lower energy beams, but the harmonics of the plasmons are too strong and obscure the weak Auger signal at such voltages. It is also worth noting that the general shape of the curve shows a near saturation of the Auger yield for incident beams of somewhere around 800 eV. This is in good agreement with the predictions of Bishop and Riviere[12] who have suggested the use of an exciting beam having 3–3.5 times the critical ionization energy of the level being studied.

Some other approximate critical ionization energies were measured. For period-4 elements we have found that less than 1.4 keV is sufficient to excite the Co transitions, while for Fe, less than 1.2 keV is sufficient. For period-5 elements, it is found that a 290-eV beam excites the Y transitions while for Ru a 400-eV beam is sufficient. Again, these values represent an upper limit to the critical ionization energies. They are probably close to the true values (except for the period-4 elements) as the discussion in Sec. IV will show.

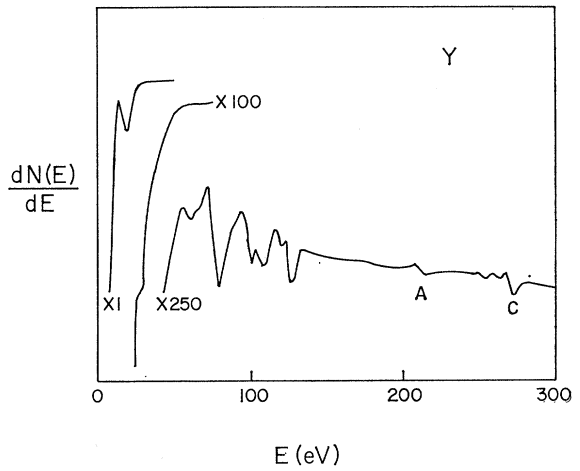


FIG. 14. Auger electron spectrum from Y foil.

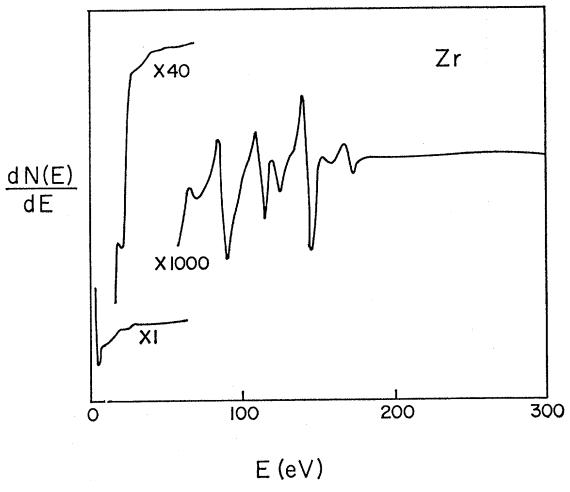


FIG. 15. Auger electron spectrum Zr foil.

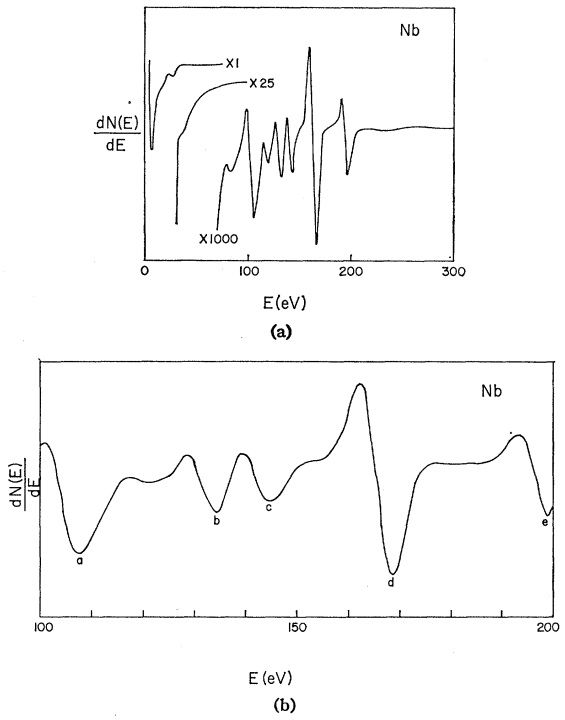


FIG. 16. (a) Auger electron spectrum from Nb (110) crystal. (b) Expanded section of (a) showing main features of the Nb spectrum in more detail. Features labeled a, b, c, etc. are discussed in text and Table III.

## IV. DISCUSSION

The correct indexing of the observed Auger transitions has not been carried out in many previous Auger electron-spectroscopy studies. This is probably because of a lack of sufficient criteria to choose between the various possible transitions. This indexing is of importance for several reasons. In the first place, any theoretical estimate of Auger transition probabilities will require evaluation of transition matrix elements of the form[21]

$$W_a=\frac{2\pi}{\hbar}\sum_{i,f}\left|\int\int\Psi_f'^*(r_1)\Psi_f^*(r_2)\times V(r_1-r_2)\Psi_i(r_1)\Psi_i(r_2)\,dr_1\,dr_2\right|^2, \quad (1)$$

where the perturbation energy $V(r_1-r_2)=e^2/|r_1-r_2|$, $\Psi_i(r_1)$ is the wave function of the first electron in its initial state, and $\Psi_f(r_1)$ is its wave function in the final state, while $\Psi_i(r_2)$ and $\Psi_f(r_2)$ are the initial and final wave functions of the second electron. This calculation obviously requires a knowledge of which electron states are involved in a particular transition. Second, if one wishes to use Auger spectroscopy to study chemical effects[14] it again is necessary to know which electrons are involved; obviously, transitions involving valence electrons will be most useful in this respect. Third, because of the large number of cases where peaks from one element overlap those of another,[17] it is important to be able to account for all observed transitions. Finally, it is possible that certain selection rules are operative which may be found by a systematic study of the observed transitions.

The criteria which we have set up to determine the proper labeling of these transitions are as follows:

(a) The calculation at which the energy of a transition will appear should be correct to within 10 eV or so using tabulated binding energies.

(b) The similarity of shape in the Auger spectra for elements in the same period of the Periodic Table suggests very strongly that the same transition is being observed in each element in a given period. With this assumption, it is necessary to assign transitions in such a way as to predict observed trends in energy with atomic number.

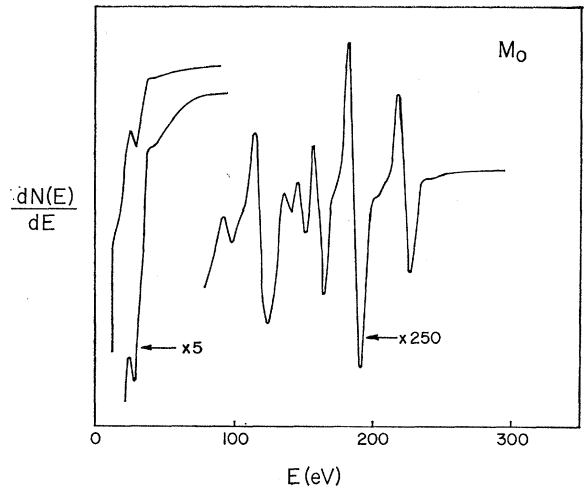


FIG. 17. Auger electron spectrum from Mo (112) crystal.

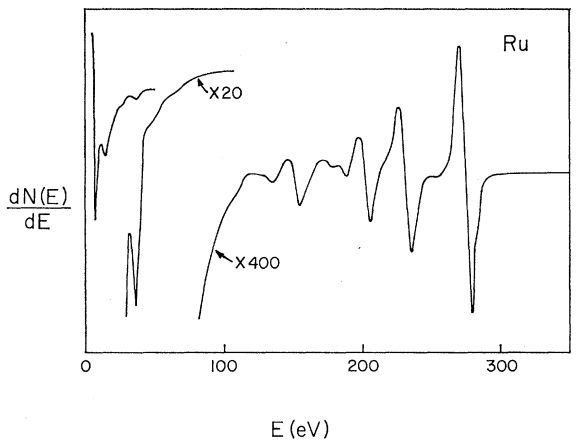


FIG. 18. Auger electron spectrum from Ru (0001) crystal.

[21] M. A. Listengarten, Izv. Akad. Nauk SSSR 24, 1041 (1960).

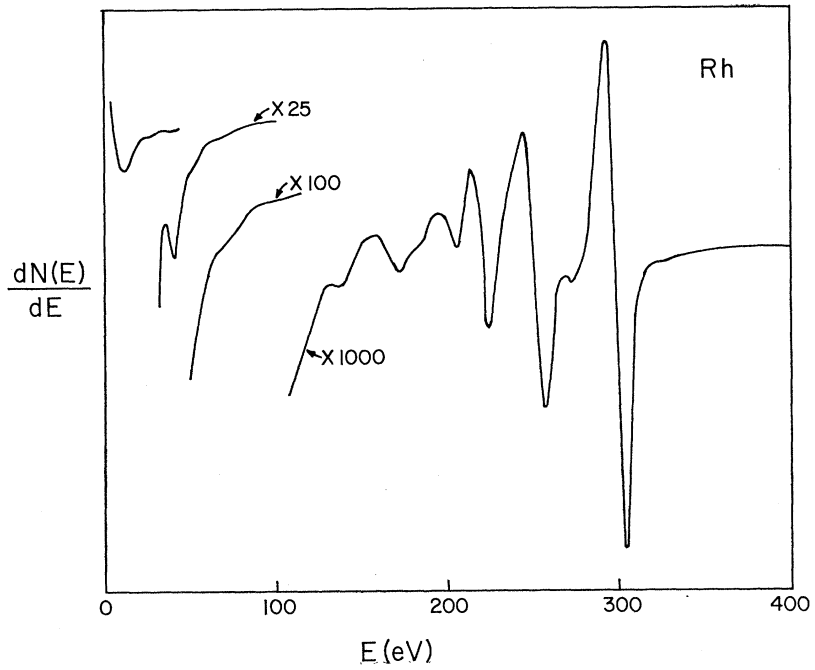


FIG. 19. Auger electron spectrum from Rh (111) crystal.

(c) Critical ionization energies set an upper limit to the binding energy for the electron energy levels which are initially ionized. The energies of the Auger electrons themselves also set a lower limit to this binding energy. This effectively limits the energy levels from which the initial ionization comes to two or perhaps three electron states.

(d) If any electrons involved in the transitions are initially from the valence bands of the element, then one might see significant changes in shape and intensity of the Auger features when the chemical state of the atom is changed, e.g., by oxidation. Such effects have not been observed in general and, hence, it is felt that most of the transitions observed here involve core electrons.

The critical ionization energies for several of the elements were discussed in Sec. III C. An inspection of the binding energies[22] for the electrons in Ta shows that the initial ionization for the 164-eV Auger transition must come from the $N_{IV}$ or $N_V$ level, using criterion (c). Thus, by using criterion (b), the transitions observed in the period-6 elements involve the initial ionization of an $N_{IV}$ or $N_V$ level.

Using similar reasoning, the transitions for elements in period 4 can be seen to involve initial ionization of an $L_I$, $L_{II}$, or $L_{III}$ level, while for period 5, these levels are the $M_{IV}$ or $M_V$ states.

The determination of these initial states results in an enormous simplification in assigning transitions. The number of possibilities is reduced further by applying criterion (a) above, as many possible transitions result in Auger electrons with energies far outside the observed range. Energies of all possible Auger transitions fulfilling the above requirements were calculated from ground-state binding energies. However, after the initial ionization of the atom, the Coulomb field causes shifting of the energy levels of the remaining electrons and one should use appropriate binding energies for excited atoms to determine Auger electron energies. Rigorously, one should calculate energies for the electronic states in these excited atoms using well-known quantum-mechanical methods.[21–26] It is, however, at best a

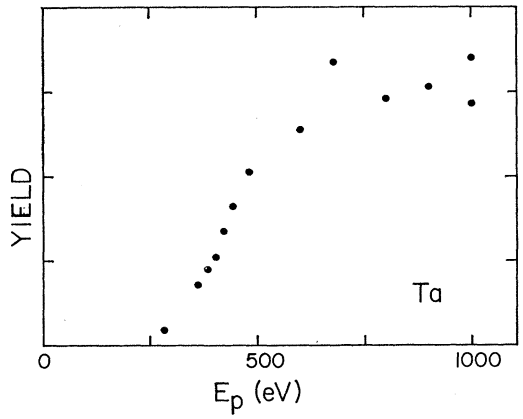


FIG. 20. Yield of Auger electrons from Ta (110) crystal as a function of incident-beam voltage. Yield is arbitrarily defined as the peak-to-peak deflection from the maximum at 164 eV to the minimum of 182 eV [see Fig. 1(b)] divided by the incident-beam current.

[22] K. Siegbahn *et al.*, Air Force Materials Laboratory Technical Report No. AFML-TR-68-189, 1968 (unpublished).

[23] G. Wentzel, Z. Physik **43**, 524 (1927).

[24] E. J. Ramberg and F. J. Richtmyer, Phys. Rev. **51**, 913 (1937).

[25] E. J. Callan, Phys. Rev. **124**, 793 (1961).

[26] W. N. Asaad, Proc. Roy. Soc. (London) **A249**, 555 (1959).

difficult task due to the lack of proper wave functions to use for these heavy metals as well as correct coupling criteria, relativistic effects, etc. In earlier work on the Auger effect, it was suggested that a good approximation to the energy could be obtained by using energy levels for the atom of next higher atomic number for the ejected electron.[27] Thus, the energy of the transition $E_{VXY}(Z)$, where $V$ is the energy level of the initial vacancy in an atom of atomic number $Z$ and the neutralizing and ejected electrons are in the $X$ and $Y$ levels, respectively, is given by

$$E_{VXY}(Z)=E_V(Z)-E_X(Z)-E_Y(Z+1). \quad (2)$$

In recent work on the Auger energies of Hg, Bergstrom and Hill[28] suggest the use of a correction factor given by

$$\Delta E=\Delta Z[E_Y(Z)-E_Y(Z+1)], \quad (3)$$

with $\Delta Z$ to be determined by experiment.

Equation (2) then becomes

$$E_{VXY}(Z)=E_V(Z)-E_X(Z)-E_Y(Z)+\Delta E. \quad (4)$$

Listengarten[21] points out that, except for $KLL$ transitions, this is probably as good a method as any for predicting Auger energies. The value of $\Delta Z$ is usually in the range[21,29] $0.5<\Delta Z<1.3$.

It has been found essential to use an equation such as (2) or (4) in correctly predicting Auger energies. The most important example of this is given by calculations for the line shape in Fig. 1(b) for elements of period 6. The possible transitions using $N_{IV}$ or $N_V$ levels for the initial vacancy were all calculated and compared with experiment. As pointed out in Sec. III B, the energy of this main Auger feature for this group of elements decreases in energy with increase in atomic number. None of the possible transitions in the appropriate energy range using ground-state binding energies exhibits this behavior. It is found, however, that using Eq. (2) does, for one particular group of transitions, predict the observed behavior. The transitions are the $N_VN_{VI}N_{VI}$, $N_VN_{VI}N_{VII}$, and the $N_VN_{VII}N_{VII}$. No other possible transitions could be found which exhibit this behavior. These data are summarized in Table I for the elements Hf to Au. An attempt to improve on the agreement between experiment and prediction was made by using the correction factor $\Delta E$ in Eq. (4), with $\Delta Z=0.7$. There was no observed improvement in the agreement over the use of $\Delta Z=1.0$ as in Eq. (2).

Several additional points in this assignment of transitions should be made. First, under high-resolution conditions, the Auger feature for these period-6 elements [see Fig. 1(b)] was found to consist of three maxima and three minima, as pointed out in Sec. III B. There are just three transitions which give the observed atomic number dependence, and their energies are very close to the experimental values (see Table I). Second, the shift in energy with atomic number is smallest for the elements Hf, Ta, and W and greatest for Ir, Pt, and Au; the calculated shifts follow this same trend. Thus, it appears as though this Auger feature can be confidently assigned as due to the $N_VN_{VI}N_{VI}$, $N_VN_{VI}N_{VII}$, and $N_VN_{VII}N_{VII}$ transitions. Strictly speaking, these transitions should be labeled as Coster-Kronig transitions,[30] as the ionized electron and the electron which neutralizes the initial hole come from the same subshell.

Similar calculations and considerations were used to assign the transitions from period-4 and period-5 elements. For the features observed with the period-5 elements [see Fig. 16(b)], the situation is somewhat more complex. Because of the slight changes in relative heights in peaks, there is some ambiguity in assignment of equivalent features. The labeling scheme shown in Table III appears the most consistent with the main transitions being $M_VN_{III}N_V$ and $M_VN_VN_V$ [these are features d and e in Fig. 16(b)]. There is more uncertainty in assigning transitions to the smaller features, a, b, and c, but again their assignment in Table III to the Auger transitions $M_VN_IN_{III}$, $M_VN_{III}N_{III}$, and $M_VN_IN_V$, respectively, gives the best over-all agreement. The use of the $\Delta Z$ rule [Eq. (3)] has little effect, since the $N$ levels for elements Z and Z+1 in this row differ by only a few eV, while the $M_{IV}$ and $M_V$ binding energies are also nearly equal.

The higher-energy transitions observed from the period-4 metals are all of the $LMM$ type. The spectrum for $V$, Fig. 11, shows that this triplet of transitions when examined under high resolution has a great deal of fine structure. The lowest-energy transition in this triplet from $V$ consists of five components. The resolution of these components requires the use of very low modulating voltages on the suppressor grid. The results from Cr were carried out before this fine structure was discovered, but it seems likely that these peaks could also be resolved into the same number of components. It is possible to identify all these $LMM$ transitions; the assignments are given in Table II. Again, the calculations were made using Eqs. (2) and (3). The use of Eq. (2) seems to give the best agreement with experiment.

The true secondary region (arbitrarily defined as those electrons having energies of $<50$ eV) also shows Auger transitions. The relevant data from these low-energy transitions is summarized in Table IV. No significant trends were found, except that perhaps more transitions are found on higher-$Z$ elements. It is possible that multiple Auger processes,[31,32] electron shake off,[33] Coster-Kronig,[30] and true Auger processes are all

[27] E. Burhop, *The Auger Effect and Other Radiationless Transitions* (Cambridge University Press, New York, 1952).
[28] I. Bergstrom and R. D. Hill, Arkiv Fysik **8**, 21 (1954).
[29] L. H. Toburen and R. G. Albridge, Nucl. Phys. **490**, 529 (1967).
[30] D. Coster and R. de L. Kronig, Physica **2**, 13 (1935).
[31] T. A. Carlson and M. O. Krause, Phys. Rev. Letters **14**, 390 (1965).
[32] M. D. Krause and T. A. Carlson, Phys. Rev. **149**, 52 (1966).
[33] M. Wolfsberg and M. L. Perlman, Phys. Rev. **99**, 1833 (1955).

involved. It seems likely that many of the Auger processes involve valence-band electrons. If this is the case then this region should be investigated more fully for chemical effects due to chemisorption as the density of states for these electrons are most apt to be affected by chemical change.

## V. SUMMARY

The Auger transitions in the intermediate-energy range for most of the transition metals in periods 4–6 have been investigated. On the basis of these results, assignments of the transitions have been made. In all cases it appears as though electrons in only the outermost shells and subshells participate in these transitions, even though incident beam energies are many times the binding energies for more tightly bound electrons. In order to calculate the Auger electron energies, it is necessary to use a correction to take account of the fact that the Auger electrons are being ejected from ionized atoms. Good agreement was obtained when using the energy levels from the next higher element for the binding energy of the ejected electron.

PHYSICAL REVIEW B VOLUME 1, NUMBER 4 15 FEBRUARY 1970

# Rigid-Band Behavior in the Specific Heats of PbTl and PbBi Alloys: Electron-Phonon Enhancement Effects*†

LAVERN C. CLUNE‡ AND BEN A. GREEN, JR.§
*Department of Physics and Condensed State Center, Case Western Reserve University, Cleveland, Ohio 44106*
(Received 7 April 1969)

The normal-state specific heats of pure lead and four dilute PbTl and PbBi alloys have been measured in the temperature range 1.0–2.3 K. The fractional rate of change of the electronic specific-heat coefficient $\gamma$ with respect to the number of conduction electrons per atom was found to be $0.25\pm0.06$ for PbTl alloys and $0.51\pm0.04$ for PbBi alloys. When changes in the electron-phonon enhancement factor as determined from tunneling measurements are included, good agreement is found between the measured changes in $\gamma$ and those expected from the rigid-band model. Semiquantitative calculations indicate that changes in the electron-phonon enhancement factor may also account for the apparent discrepancy between previous experimental results and the rigid-band model in noble-metal alloys. The Debye temperature was found to decrease for both lead alloy series.

## INTRODUCTION

THE electronic specific heats of simple alloys of the noble metals have puzzled investigators ever since it became known that the Fermi surface of copper makes contact with the first Brillouin-zone boundary. For Rayne[1] had found that addition of Zn to Cu increases the coefficient of the linear term in the specific heat, which is proportional to the density of electron states at the Fermi energy, and it was thought that adding Zn should merely increase the Fermi energy without seriously distorting the shape of surfaces of constant energy. Most calculations of the band structure of Cu, however, agree that the density of states should decrease with energy for energies beyond that at which said contact occurs.[2,3]

Examples of this phenomenon have since multiplied to include several alloy systems based upon each of the noble metals[4–13] in an attempt to explore the effects of solute valence, size, and mass on the rate of increase of $\gamma$ with concentration. Size of the solute atom appears to have little to do with the rate of increase, while both valence and mass are significant variables. (Although atomic mass and size are strongly correlated, giving rise to ambiguity of interpretation, the comparison of

* Manuscript preparation supported by National Science Foundation Departmental Science Development Grant No. GU 2603 to Ohio University.
† Part of a thesis by L. C. C. submitted to Case Western Reserve University in partial fulfillment of the requirements for the Ph.D. degree.
‡ National Defense Education Act Fellow during part of this research. Present address: Ohio University, Athens, Ohio 45701.
§ Present address: Massachusetts Institute of Technology, Cambridge, Mass. 02139.
[1] J. A. Rayne, Phys. Rev. **108**, 22 (1957). These results were probably slightly in error because of paramagnetic impurities but the increase (although smaller) was confirmed by B. W. Veal and J. A. Rayne [*ibid.* **130**, 7156 (1963)] and by L. C. Clune and B. A. Green, Jr. [*ibid.* **144**, 525 (1966)].
[2] J. M. Ziman, Advan. Phys. **10**, 1 (1961).
[3] J. S. Faulkner, H. L. Davis, and H. W. Joy, Phys. Rev. **161**, 656 (1967).
[4] B. A. Green Jr. and H. V. Culbert, Phys. Rev. **137**, A1168 (1965).
[5] H. Montgomery, G. P. Pells, and E. M. Wray, Proc. Roy. Soc. (London) **A301**, 261 (1967).
[6] L. C. Clune and B. A. Green, Jr., Ref. 1.
[7] B. A. Green, Jr., Phys. Rev. **144**, 528 (1966).
[8] T. A. Will and B. A. Green, Jr., Phys. Rev. **150**, 519 (1966).
[9] L. J. Badar and B. A. Green, Jr., Bull. Am. Phys. Soc. **12**, 20 (1967).
[10] B. A. Green, Jr., and H. M. Wu (to be published).
[11] B. A. Green, Jr., and A. A. Valladares, Phys. Rev. **142**, 374 (1966).
[12] H. J. Blythe, T. M. Holden, M. Dixon, and F. E. Hoare, Phil. Mag. **11**, 235 (1965).
[13] D. A. Dicke and B. A. Green, Jr., Phys. Rev. **153**, 800 (1967).